

## A Readable Chromatic Biosensor with a Tunable Detection Threshold

Chiao-Hsiu Tsai, Ying-Jhan Hong, Jing-Huei Huang, Pin Chang and Tri-Rung Yew\*

Department of Materials Science and Engineering, National Tsing-Hua University, Hsinchu 30013, Taiwan

### Abstract

Rapid and readable chromatic detection of antigen is essential for medical and clinical applications as they are inexpensive, portable and simple in operating process. In addition, results from chromatic biosensors can be easily readout without any equipment or instrument collocation. However, only a few studies accomplished the goal by detecting the antigen via this strategy; even though, the detection range is still narrow and only could be applicate on some specific disease identification. Still, most of the chromatic biosensors are continuing color transition and hard to identify the disease at critical point. Therefore, it is essential to develop a wide-detecting ranged or detecting range tunable chromatic biosensor revealing considerably color-change for numerous diseases recognition. This article presents a detection range tunable readable chromatic biosensor for antigen detection, demonstrated by the detection of human serum albumin (HSA). First, the HSA sample was pre-conjugated to chitosan to form HSA-chitosan complex, then, the HSA-chitosan complex was utilized to synthesize Ag NPs. According to the color shown by the synthesized Ag NPs, 0.01-0.3 mg/ml HSA sample could be determined. Furthermore, the detection range could be adjusted to 0.001-0.1 or 0.1-1 through decreasing or raising the chitosan-conjugating concentration, showing the potential for more disease identification application.

**Keywords:** Chromatic biosensor; Silver nanoparticle; Chitosan; Human serum albumin; Indicative

### Introduction

Chromatic biosensors based on the correlation between the antigen concentration and the color of the readout has drawn considerable attention in clinical diagnosis and treatment [1]. Moreover, chromatic methods are extremely attractive because they are inexpensive, portable and simple in operating process. Even more, results from chromatic biosensors can be easily recognized without using any instrument or equipment.

Many studies have been focused on adopting chromatic methods for detecting DNA, proteins, small molecules and ions [2-4]. For example, Lee et al. used the aggregation of carbon nanotubes (CNTs) to detect nucleic acid and achieved the detection limit of  $10^{-12}$  M [5]. Lim et al. used Au NPs to sense glucose in blood and reported the detection limit of  $2 \times 10^{-3}$  M [6]. Daniel et al. used Au NPs to sense  $\text{NO}_2^-$  ions and observed obviously color change near the concentration of  $2.17 \times 10^{-5}$  M [7]. However, the detection range is still narrow and only could be applied on some specific disease detecting or bio-molecule sensing application. Therefore, it is significant to develop a wide detecting-ranged or detection range tunable chromatic biosensor for disease-identifying application [8-10].

Many diseases including cancers could be detected by analyzing the quantity of the specific proteins [11,12]. For example, liver and kidneys are the major organs in the human body, and HSA is a well-known biomarker of liver and kidney functioning [13]. When HSA concentration of  $>0.02$  mg/mL in urine implies that the patient may suffer from kidney-related disease. On the other hand, when HSA concentration of  $<30$  mg/mL in blood implies that the patient may take liver-related disease [14,15]. Through designing the chromatic biosensors which the detection ranges are fit with the disease-indicating concentration, patients can know their conditions in time by themselves from the chromatic biosensors and therefore can take early medication care before the disease becomes fatal, thereby enhancing the probability of saving their lives. To sum up, it is urgently needed to establish chromatic methods for antigen-detecting use, and make the chromatic threshold to match plentiful disease-indicator for disease-identifying applications.

In this study, HSA was selected as the detection target as it is a biomarker of the health of liver and kidney function. The HSA with various concentrations was conjugated to chitosan to inhibit its ability of synthesizing Ag NPs. Chitosan was used as a template for conjugating HSA because it showed great biocompatibility and capability of synthesizing Ag NPs [16,17]. In addition, Ag NPs exhibit surface plasmon resonance effect [18], which induced color as a readout. Furthermore, the detection range could be adjusted by tuning the chitosan concentration. It is expected the detection range could be adjusted so as to demonstrate the feasibility of using the aforementioned chromatic approach for other disease-identification applications.

### Materials and Methods

#### Simple chromatic biosensing system

The fabrication of the chromatic biosensor is shown in Scheme 1. It comprised three main processes, including the (a) preparation of a sensing solution, i.e., chitosan solution (Scheme 1a), (b) conjugation of HSA to the surface of chitosan (Scheme 1b) and (c) synthesis of Ag NPs for readout and to quantify the HSA concentration (Scheme 1c). These processes are briefly described as follows.

#### Antigen conjugation and Ag NPs synthesis

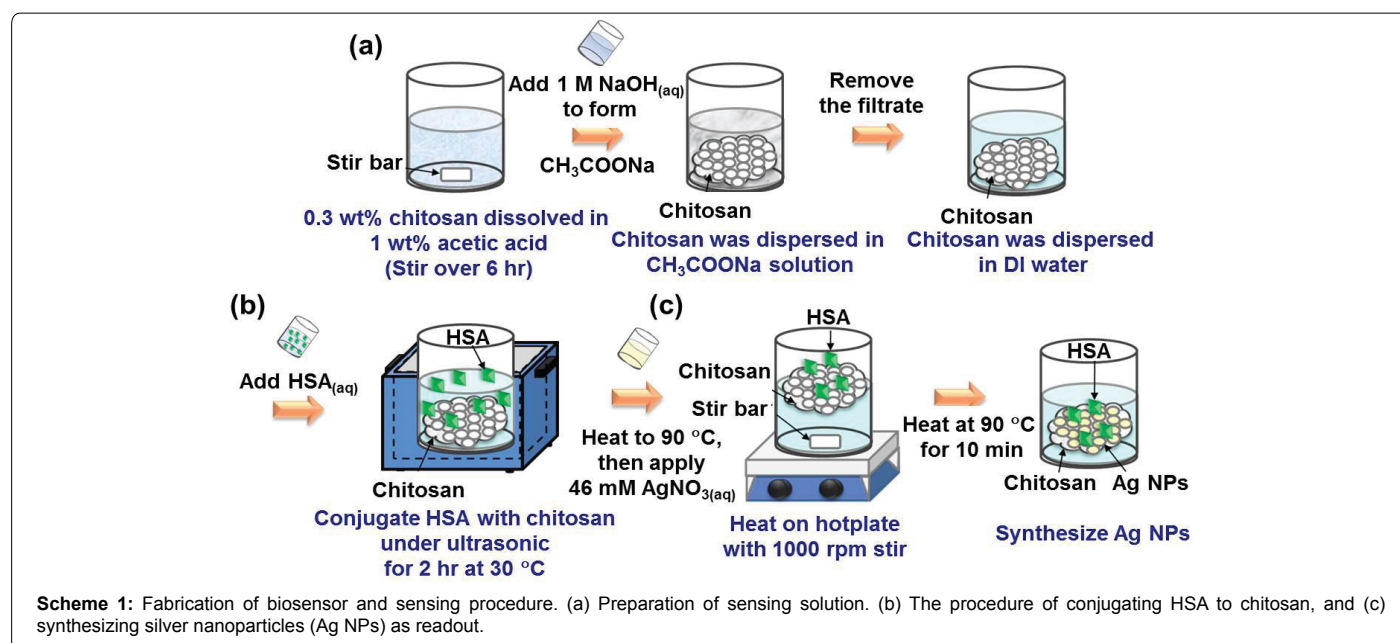
First, the sensing solution was prepared by dispersing chitosan in de-ionized water. Chitosan powder (100–300 kDa) was dissolved in 1 wt% acetic acid ( $\text{CH}_3\text{COOH}$ ) for preparing 0.3 wt% chitosan solution. Furthermore, with stirring over 6 h, 1 M NaOH was added to the chitosan solution to disperse chitosan in  $\text{CH}_3\text{COONa}$  solution at the

\*Corresponding author: Tri-Rung Yew, Department of Materials Science and Engineering, National Tsing-Hua University, Hsinchu 30013, Taiwan, Tel: +886-936347230; Fax: +886-3-5722366; E-mail: [tryew@mx.nthu.edu.tw](mailto:tryew@mx.nthu.edu.tw)

Received July 25, 2016; Accepted August 21, 2016; Published August 28, 2016

Citation: Tsai CH, Hong YJ, Huang JH, Chang P, Yew TR (2016) A Readable Chromatic Biosensor with a Tunable Detection Threshold. J Microb Biochem Technol 8: 390-394. doi: 10.4172/1948-5948.1000314

Copyright: © 2016 Tsai CH, et al. This is an open-access article distributed under the terms of the Creative Commons Attribution License, which permits unrestricted use, distribution, and reproduction in any medium, provided the original author and source are credited.



1 M NaOH to chitosan solution volume ratio of 3:10. Then, the filtrate was removed by centrifugation for three times to get rid of the ions in the solvent. Following that, the HSA dissolved in de-ionized water was added to the sensing solution, and kept in an ultrasonicator at 30°C for 2 h to conjugate HSA with chitosan.

The HSA-conjugated chitosan solution was then heated in a water bath at 90°C followed by adding 46 mM silver nitrate ( $\text{AgNO}_3$ ) in water at a volume ratio of 1:1, with the reaction temperature maintained at 90°C for 10 min to synthesize Ag NPs. Finally the color of Ag NPs solution was used as the readout to quantify the HSA concentration.

## Results and Discussion

### Sensing result on chromatic diagram

To correlate the color of synthesized Ag NPs with HSA concentration, the color of Ag NPs synthesized by various HSA-chitosan complexes was shown in Figures 1a-1c. First, various colors of the synthesized Ag NPs were summarized based on the chromatic diagram of 2-deg with D65 (Figure 1a). The chromaticity of a color was then specified by the two derived parameters  $x$  and  $y$ . The synthesized Ag NPs ranged from  $x=0.3$  to  $x=0.6$  and  $y=0.3$  to  $y=0.5$  (Figure 1b). The color of Ag NPs changed from yellow to grey when a higher concentration of HSA was conjugated to chitosan as observed in Figure 1b. Furthermore, the color was almost the same at <0.01 mg/mL of HSA, while changed drastically at 0.01–0.3 mg/mL of HSA. To quantify the correlation between the color of the Ag NPs and the HSA concentration, the distance between the color of the Ag NPs and the white point, set at (0.3127,0.3290), was calculated and defined this distance as the chromaticity difference. Figure 1c shows the correlation between the HSA concentration and the chromaticity difference. In Figure 1c, the synthesized Ag NPs exhibited dark brown, yellow, and gray color, when the HSA concentration was at <0.02 mg/mL, 0.02 mg/mL ~ 0.01 mg/mL and >0.3 mg/mL, respectively. The color change from dark brown (<0.02 mg/mL) to yellow or gray at >0.02 mg/mL could be used for detecting kidney-related diseases, as an HSA concentration of >0.02 mg/mL in urine implies the patient suffers from kidney-related disease.

### UV-Vis and TEM analysis of synthesized Ag NPs

The synthesized Ag NPs were analyzed using ultraviolet-visible (UV-Vis) and their transmission electron microscopy (TEM) was shown in Figure 2 to investigate the relationship of HSA concentrations versus Ag NPs colors. The absorption spectra analyzed by UV-Vis were shown in Figures 2a and 2b, which exhibited characteristic peaks at approximately 420 nm, except for the Ag NPs synthesized using 0.3 mg/mL HSA. According to Figure 2a, the absorbance spectra of the Ag NPs synthesized using 0–0.01 mg/mL HSA were similar. As the HSA concentration increased from 0.01 to 0.1 mg/mL, the intensity of the absorbance spectra decreased, implying the reduction of Ag NPs. In additions, in order to compare the chromatic difference of Ag NPs easily, the absorbance-to-wavelength spectrum shown in Figure 2a was converted to the absorption-to-wavelength spectrum as shown in Figure 2b. In this way, the most obvious difference in color could be observed from the samples with the HSA concentration ranging from 0.1 to 0.3 mg/mL, which shows the same trend as observed in Figure 1c.

The TEM analysis was also conducted on synthesized Ag NPs for the further correlation between synthesized Ag NPs and HSA concentrations. The TEM images of the Ag NPs synthesized using 0, 0.1 and 0.3 mg/mL HSA are shown in Figures 2c-2e, respectively. The number of Ag NPs (at the same volume of solution) decreased at higher HSA concentrations. Therefore, the conjugation of HSA to chitosan is assumed to inhibit the reactivity of chitosan for synthesizing Ag NPs. Furthermore, it is considered that HSA occupies the reaction site of chitosan so as to inhibit the Ag NPs synthesis reaction. The size distribution and surface density of the synthesized Ag NPs were estimated by analyzing the TEM images and the result were presented in Figures 2f-2h, respectively. From Figures 2f-2h, the surface density of the Ag NPs synthesized without using HSA was 83.4 #/μm<sup>2</sup>, and decreased to 41 #/μm<sup>2</sup> for those using 0.1 mg/mL HSA, and further decreased to 10.6 #/μm<sup>2</sup> using 0.3 mg/mL HSA. Moreover, the size of the Ag NPs was approximately <40 nm as they were synthesized without using HSA as shown in Figures 2c and 2f, which exhibited dark brown color (Figure 1c) due to high surface density (83.4 #/μm<sup>2</sup>). From Figures 2d and 2g, the surface density of Ag NPs synthesized using 0.1

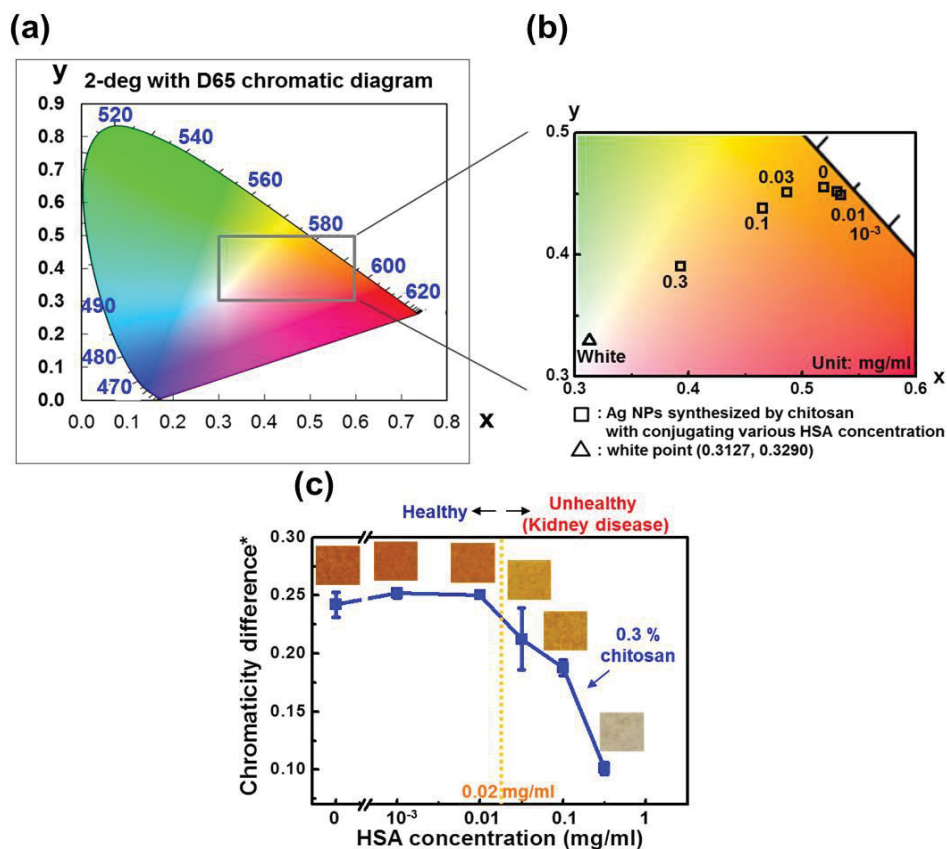


**Figure 1:** (a) The chromatic diagram of 2-deg with D65. (b) The colors of Ag NPs reduced from chitosan conjugated with various concentrations of HSA on the chromatic diagram. (c) The plot to correlate chromaticity difference versus HSA concentration, with the colors of Ag NPs inserted. Chromaticity difference\*: The distance of each point on the chromatic diagram to the white point (0.3127, 0.3290).

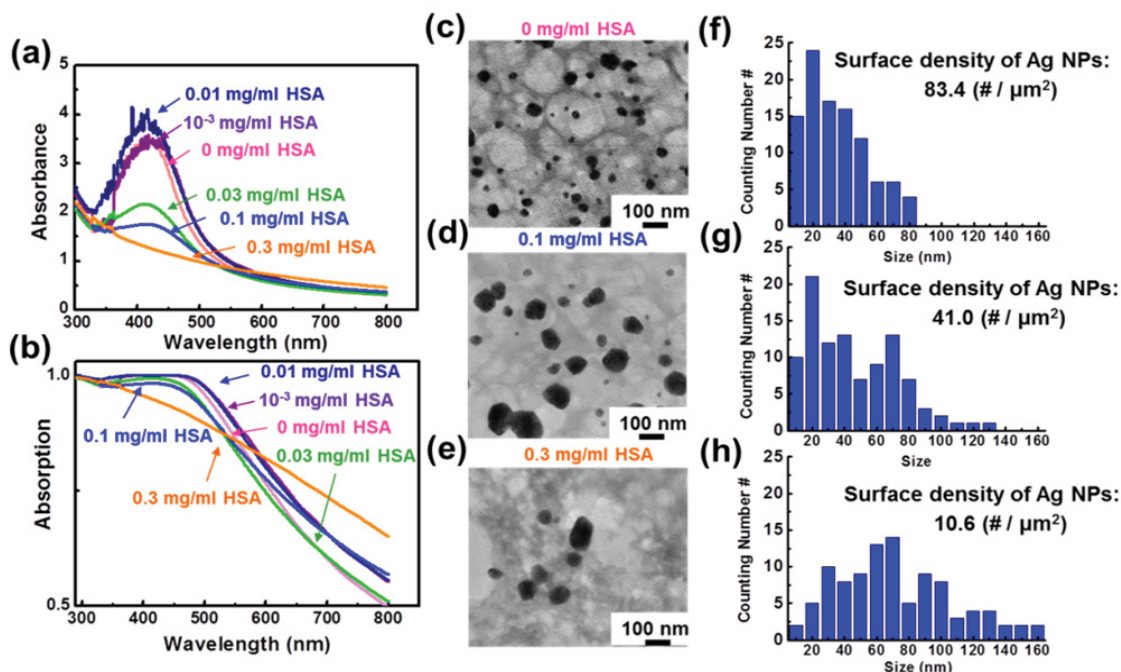


**Figure 2:** The UV-Vis analysis of Ag NPs reduced by chitosan conjugated with various concentrations of HSA, showing the results of (a) absorbance versus wavelength, (b) absorption versus wavelength. The TEM bright field image of Ag NPs reduced by chitosan conjugated with (c) 0 mg/ml, (d) 0.1 mg/ml, and (e) 0.3 mg/ml HSA and their respective size distribution and surface density in (f), (g) and (h), respectively.

mg/mL HSA decreased to 41 #/μm<sup>2</sup> and the quantity of Ag NPs size >40 nm increased compared to the Ag NPs synthesized without using HSA (Figure 2f). In additions, at a decreased density and smaller size of Ag NPs, the peak of UV-Vis spectra would become smaller and broader, as observed in Figure 2a. For Figure 2e and 2h, the surface density of Ag NPs synthesized using 0.3 mg/mL HSA decreased to 10.6 #/μm<sup>2</sup> and the size distribution was approximately 60–100 nm (Figure 2h). Furthermore, when the density of Ag NPs decreased and the size of Ag NPs were about 60–100 nm, the peak of spectra for surface plasmon resonance in UV-Vis became hard to be observed (Figure 2a). For the preceding analysis, it is known that the density of synthesized Ag NPs would further decrease and the quantity of larger-sized Ag NPs will increase, when the higher concentration of HSA was used to conjugate with chitosan.

### Tuning the sensing region by changing chitosan concentration

Figures 3a and 3b shows normalized chromaticity difference measured from the UV-Vis spectra and the color of Ag NPs synthesized by HSA-conjugated chitosan with three different concentrations of chitosan. In order to investigate the feasibility of tuning chromatic threshold of the Ag NPs synthesized by HSA-conjugated chitosan, three chitosan concentrations, 0.12 wt%, 0.3 wt%, and 0.9 wt%, were used with the result shown in Figure 3a. The chromaticity difference at a point without HSA conjugation was defined to be 100%, and at the point in the UV-Vis spectra without any peak observed was defined to be 0%. Moreover, all experiments under these conditions were repeated for three times. As observed in Figure 3a, the curves of normalized chromaticity difference versus HSA concentration for the solutions with 0.12% and 0.9% chitosan exhibited a shift to the left and right, respectively, compared to that with 0.3% chitosan. The colors of Ag NPs synthesized using various chitosan and HSA concentration could be observed in Figure 3b. When 0.9% chitosan was used, the color changed from brown to black at 0.1–1 mg/mL of HSA, while from dark brown to gray at 0.01–0.3 mg/mL of HSA using 0.3% chitosan. Besides, when 0.12% chitosan was used, the color changed from light yellow to white at 0.001–0.1 mg/mL of HSA. Thus, the color transition of Ag NPs at different HSA concentration detection range for three chitosan concentration implies that the detection range of this biosensor could be controlled by tuning the chitosan concentration.

### Advantages of this work

The comparison of this work with previous studies is as following.

Fengli Qu et al. combined the advantage of graphene oxide and magnetic ball to detect PSA (Prostate Specific Antigen). The detection range is  $1 \times 10^{-7}$ – $1 \times 10^{-5}$  mg/ml and the color is changed from black to brown [19]. For the work from Xiuli Fu et al., quenching effect of graphene oxide was applied on gold nanorod to detect Heparin. The detection range is  $2.0 \times 10^{-5}$ – $2.8 \times 10^{-4}$  mg/ml and the color is changed from blue to colorless [20]. Both of the previous work showed that the detection range of the typical chromatic biosensor are within 1 to 2 orders. The application of chromatic biosensor is still difficult due to its narrow detection range, even though it shows the obvious color-changing ability.

The chromatic biosensor developed in this work shows the advantage of the obvious color change from brown, yellow to grey when the concentration of sensing target is applied from  $10^{-2}$  to  $3 \times 10^{-1}$  mg/ml. Furthermore, the detection range of this chromatic biosensor could be changed to  $10^{-3}$  to  $10^{-1}$  and  $10^{-1}$  to 1 when tuning the chitosan concentration to 0.12% and 0.9%, respectively. Finally, the success of using HSA as a sensing target to demonstrate the feasibility of the sensing mechanism developed in this work can be implemented to sense liver and kidney diseases in the future and provide the potential application to other protein biomarkers.

### Conclusion

A new approach of chromatic biosensor has developed for detecting HSA concentrations through the synthesis of Ag NPs using HSA-conjugated chitosan, which could be leveraged for the applications of disease-identification. Using 0.3 % chitosan as a reducing agent, the color of Ag NPs synthesized by HSA-conjugated chitosan exhibited dark brown, yellow and gray color, when the HSA concentration was at <0.02 mg/mL, 0.02–0.01 mg/mL and >0.3 mg/mL, respectively. The color change from dark brown (<0.02 mg/mL) to yellow or gray (>0.02 mg/mL) could be used for detecting kidney-related diseases. The UV-Vis and TEM results revealed that the less and bigger Ag NPs were synthesized at higher HSA concentrations, which could result in different color readout. Moreover, the detection range of HSA concentrations (originally 0.01–0.3 mg/mL) could be changed to 0.001–0.1 or 0.1–1 mg/mL by adjusting the chitosan concentration to 0.12% and 0.9%. In conclusion, by using this strategy, the biosensor could be applied to detect numerous diseases simply through direct observation of color change. With further investigation on actual serum samples, interference, and stability, this biosensor exhibits high potential for daily usage of disease detection.

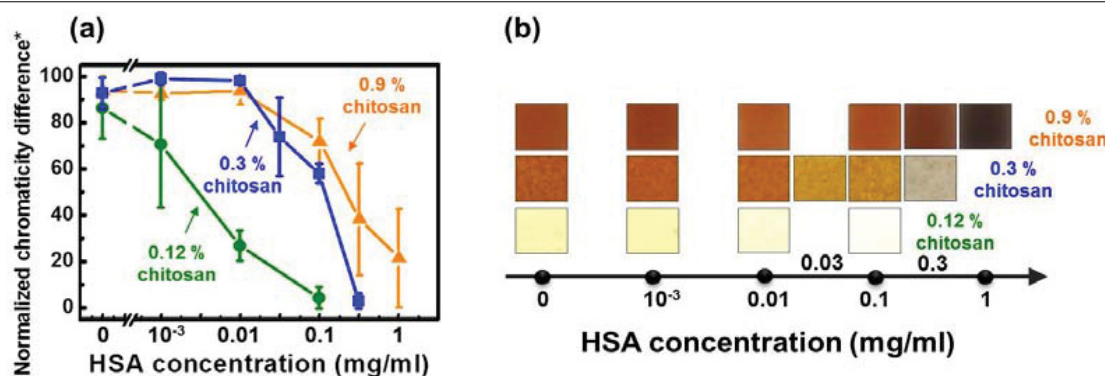


**Figure 3:** (a) The normalized plot of chromaticity difference versus HSA concentration using 0.12%, 0.3%, 0.9% chitosan concentrations for the conjugation with HSA. (b) The photograph and color of Ag NPs versus HSA concentration at various chitosan concentrations. Chromaticity difference\*: The distance of each point on the chromatic diagram to the white point (0.3127, 0.3290). Normalized chromaticity difference\*: The chromaticity difference without HSA conjugation was defined to be 100% and UV-Vis spectra at which no peak was observed was defined to be 0%.

## Acknowledgement

This work was supported by National Science Council under project numbers NSC100-2221-E-007-022-MY3. The authors thank the facility support by NTHU.

## References

1. Agasti SS (2010) Nanoparticles for detection and diagnosis. *Advanced Drug Delivery Reviews* 62: 13.
2. Liu D (2011) Gold nanoparticles for the colorimetric and fluorescent detection of ions and small organic molecules. *Nanoscale* 3: 1421-1433.
3. Lee K (2010) Recent advances in fluorescent and colorimetric conjugated polymer-based biosensors. *Analyst* 135: 2179-2189.
4. Shen (2014) recent development of sandwich assay based on the nanobiotechnologies for proteins, nucleic acids, small molecules and ions. *Chemical reviews* 114: 7631-7677.
5. Lee (2007) Carbon nanotube-based labels for highly sensitive colorimetric and aggregation-based visual detection of nucleic acids. *Nanotechnology* 18: 455102.
6. Lim (2013) Gold glyconanoparticle-based colorimetric bioassay for the determination of glucose in human serum. *Microchemical Journal* 106: 154-159.
7. Daniel (2009) Colorimetric nitrite and nitrate detection with gold nanoparticle probes and kinetic end points. *Journal of the American Chemical Society* 131: 6362-6363.
8. Zeng S (2011) A review on functionalized gold nanoparticles for biosensing applications. *Plasmonics* 6: 491-506.
9. Cao J (2014) Gold nanorod-based localized surface plasmon resonance biosensors: A review. *Sensors and Actuators B: Chemical* 195: 332-351.
10. Holzinger M (2014) Nanomaterials for biosensing applications: A review. *Frontiers in Chemistry* 2: 1-10.
11. petricoin ef (2002) Clinical proteomics: Translating benchside promise into bedside reality. *Nature Reviews Drug Discovery* 1: 683-695.
12. Kumar M, Sarin SK (2009) Biomarkers of diseases in medicine. *Indian Academy of Sciences Bangalore India* 403-417.
13. Kragh-hansen U (2002) Practical aspects of the ligand-binding and enzymatic properties of human serum albumin. *Biological and Pharmaceutical Bulletin* 25: 695-704.
14. Curry S (1998) Crystal structure of human serum albumin complexed with fatty acid reveals an asymmetric distribution of binding sites. *Nature Structural Biology* 5: 827-835.
15. Ha CE (2009) Effects of statins on the secretion of human serum albumin in cultured HepG2 cells. *Journal of Biomedical Science* 16.
16. Rinaudo M (2006) Chitin and chitosan: Properties and applications. *Progress in Polymer Science* 31: 603-632.
17. Wei D (2010) Chitosan as an active support for assembly of metal nanoparticles and application of the resultant bioconjugates in catalysis. *Carbohydrate Research* 345: 74-81.
18. Wiley BJ (2006) Maneuvering the surface plasmon resonance of silver nanostructures through shape-controlled synthesis. *The Journal of Physical Chemistry B* 110: 15666-15675.
19. Qu F, Li T (2011) Colorimetric platform for visual detection of cancer biomarker based on intrinsic peroxidase activity of graphene oxide *Biosensors and Bioelectronics* 26: 3927-3931.
20. Fu X, Chen L (2012) Label-free colorimetric sensor for ultrasensitive detection of heparin based on color quenching of gold nanorods by graphene oxide *Biosensors and Bioelectronics* 34: 227-231.